Hygric behavior of building materials and their influence on indoor environment

Master Thesis

Magnus Bøgh Enevoldsen
Michał Nowak

Department of the Built Environment, Aalborg University, Aalborg, DK

Building Energy Design
Department of the Built Environment
Thomas Manns Vej 23
Dk-9220 Aalborg Ø
Denmark
Phone: +45 9940 8484
E-mail: civil@civil.aau.dk

Title:
Hygric behavior of building materials and their influence on indoor environment.

Semester:
4th semester

Project period:
Autumn Semester, 2020

Supervisors:
Kirstine Meyer Frandsen,
Rasmus Lund Jensen

Project group:
Michał Nowak,
Magnus Bøgh Enevoldsen

Page Numbers:
16 + Appendix

Date of Completion:
8th January 2021

Acknowledgment:

The authors wish to thank Valentin Gruber from Skamol A/S company for the possibility of cooperating during this project. Especially, the help and guidance during laboratory work and information about Skamol products. Furthermore, we want to appreciate his time spent during samples measurement every day and supporting us with data. We also want to thank our supervisors, Kirstine Meyer Frandsen and Rasmus Lund Jensen for their advice and assistance throughout this project.

Hygric behavior of building materials and their influence on indoor environment

Magnus Bøgh Enevoldsen[1], Michal Nowak[1]

Department of the Built Environment, Aalborg University, Aalborg, DK

Abstract

Growing interests in indoor environment and requirement of low-energy consumption buildings indicates needs for solution of a passive regulator. Following thesis focuses on on-site measurements of thermal and hygric parameters of materials along with analysing their passive influence on indoor environment, via dynamic simulation (BSim software), with greater attention to indoor relative humidity. Undertook measurements are sorption isotherms, thermal diffusivity, specific heat capacity and two ways of deriving moisture permeability. Two hemp-lime building materials and two Skamol products are analysed, along with three different interior renders. Calculations are made on moisture buffer values and retardation factor is determined between two moisture permeability methods. The outcome of the study presents great moisture buffering performance of hempcrete and calcium silicate products, while breathable renders are to some extent limiting moisture permeability. Application of hygric materials on modern constructions in dynamic simulation presents improved indoor relative humidity with lower moisture fluctuations compared with construction with none or low hygric properties.

Keywords – Hygric building materials, indoor environment, Moisture Buffer Value, indoor renders, dynamic simulation, laboratory measurements.

I. Introduction

With the increasing number of spending time indoors (around 90 [%] daily), indoor environment contributes utmost to people's well-being, health, and performance [1] [2] [3]. Despite recently greater interest in issues related to indoor air quality (IAQ) and the effect on health and productivity of occupants, the number of complains is unchanged over the years.

Previous solutions to improve IAQ are mechanical ventilation and low emitting building materials. [4]. Large thermal resistance and almost total airtightness of modern constructions, to reduce heat dispersions by construction and infiltration, leads to a large moisture loads variations (very low and high relative humidity) in building interiors. [2]. That paradoxically leads to a larger energy consumption by controlling the indoor environment and moisture via mechanical units [5].

However, passive ways of moderating the moisture loads are also present. Hygric materials are proven to improve environment in various cases and constructions [6] [7]. Capillarity of these porous materials allow to moderate humidity levels indoors, and so their hygric properties to store water particles, passively interfering with surrounding, hence acting as moisture buffer [8] [9]. According to [10], solution applied to building with mechanical HVAC equipment expects to decrease energy consumption for heating (up to 5 [%]) and cooling (up to 30 [%]).

Hygric properties of building materials have been experimentally investigated, where material scale testing including sorption isotherms, vapor permeability and moisture buffer value has provided more awareness in the industry. Some biobased, hygric constructions materials are cotton stalks, straws and hempcrete, to name a few [11] [12]. The last mentioned one can be utilized as an outright system for most of the building elements (external and internal walls, roofs).

Hemp and lime materials has proven to have excellent hygric properties to passively regulate temperature and humidity [13] and have a low impact on the environment due to their carbon storage and low embedded energy. The element is made of hemp shiv and a lime-based binder. Depending on the composition it can be used for numerous applications.

Both thermal and hygric properties been investigated in previous studies resulting in good thermal properties where thermal conductivity ranges from 0.086 to 0.138 [W/m*K] [14] [15] and specific heat capacity of 1000 to 1560 [J/kg K] [14] [16] [17]. Furthermore, the materials hygric properties has showed hysteresis on sorption curves throughout the total range of RH [18] and high water vapor permeability [14] [18] due to its open porosity [19]. The moisture buffer value has also been investigated by [11] [20] [18] [21], and according to the classification of the NORDtest protocol the result in the classification as good or excellent with outcomes of 1.94 to 3.47 [g/m²%RH] of moulded hempcrete, 2.08 to 2.22 [g/m²%RH] of sprayed hempcrete and 1.23 to 1.64 [g/m²%RH] of hempcrete render. The properties vary from different formulations, densities, and water content, where materials with lower binder ratio have better thermal conductivity but lower strength and stiffness.

Materials that are also used to regulate moisture from the indoor environment passively are two products from Skamol A/S company - calcium silicate (CaSi) and Moler (diatomaceous earth / clay) bricks, which can be applied as internal cladding in already existing envelope [22] [23]. Porous CaSi board was initially a solution for wet basements and renovation projects to maintain external historical façade. Although CaSi is known in renovation projects, utilization of such material in modern building is not widely common. Moler brick presents lower density than usual brick (700kg/m3 instead of around 1700 kg/m3) and with diatoms have fine, delicate framework with multiple micropores giving the product excellent insulation properties (0.015 [W/m*K]). These two specific material were not broadly evaluated in various research papers, however, they are commercially available and documented outcome of utilizing those materials are tackling problems with damp interior: reduction of cold wall sensation, prevention of mould growth in old buildings and lowering energy consumption [22] [23] [24]. Some of their thermal and hygric properties are known, presented in Section A.2. Both materials with their properties are expected to moderate moisture indoors in modern buildings struggling with RH. [11].

Following paper aims at investigating hygric behaviour of presented materials. These are: two types of hemp-lime materials with mixing ratios formulated by AAU [25] and two products from Skamol company (CaSi and Moler brick). Firstly, on-site material scale measurements will be performed to derive some hygric and thermal properties of the materials. These are specific heat capacities, thermal diffusivity, sorption isotherms, two ways of determining moisture permeability and moisture buffer value. Some of the measurement outcomes will be insert into dynamic simulation (BSim software) to examine their effect on indoor environment (with focus on moisture buffering performance) and compare with conventional building materials. Lacking parameters will be assessed via literature.

Traditional method of determining moisture permeability (ability of water vapor passing through pores in the material) is the Wet cup / Dry cup method [26] [27]. It is known to be time-consuming due to natural airflow from controlled surrounding via specimen to area with 0 [%] RH (absorbed by aqueous solution) [28]. Alternative measurement can be conducted by ODA20 device using N2 to remove oxygen in a chamber below sample and reducing measurement time to several hours. However, document from [29] states that due to forced flow dismissing capillary, condensation, sorption, and surface diffusivity the result differs from traditional method and hence retardation factor is needed to adopt the outcome in in further research.

Another parameter which presents materials moisture properties in a holistic way is Moisture Buffer Value (MBV) [30] [31]. MBV demonstrates moisture rate flow of investigated material surface area during various humidity activity surrounding specimen and it is determined via NORDtest protocol. While practical way ($MBV_{practical}$) is based on on-site measurement, theoretical way (MBV_{ideal}) presents moisture effusivity as main parameter, including error of steady-state analysis. MBV will be hence additionally calculated and analysed to properly describe tested materials properties.

Lastly, influence of internal plaster on moisture buffering performance will be investigated. Indoor renders are often applied on construction, but it is important to have them abrasion-resistant and breathable. These coatings are frequently gypsum or lime based [32]. Already in 1960 Künzel [33] started to investigate plasters moisture influence on indoor environment, however there is still possibility of disregarding that building element, creating risk of applying plaster without sorption properties, devastating whole moisture buffering ability of a building. Including render in building design is hence utmost important. Following paper will present three different plasters and their abilities followed by measurement of oxygen diffusion coefficient.

II. Materials & Methods

A. Materials

1. Hempcrete

Compositions and manufacturing

The study includes two hempcrete mixtures, one for walls application high-hemp mixture (HH) and another low-hemp (LH) for render. Table 1 gives the proportions of the mix and the manufacturing method of the two variations. The mixing method is performed according to [25] where firstly slaked lime is produced form CaO and water, after which hemp shiv, hydrated lime, fly ash and sand (only in LH) are added to the mix. Detailed description is presented in Appendix A.

Materials Properties

Thermal and hygric properties of HH and LH have been tested by Aalborg University (AAU), which properties are comparable to other hemp / lime constructions [25] & [29] although the materials have different density and mixing ratios. Thermal and hygric properties can be seen in Table 2.

Table 1 - Hempcrete mixing ratios

HH - Binder ratio by mass				
Hydrated lime	**Hydraulic lime**	**Fly ash**	**Hemp/ Binder**	**Water/ Binder**
75%	15%	10%	0.5	3

LH - Binder ratio by mass					
Hydrated lime	**Hydraulic lime**	**Fly ash**	**Sand**	**Hemp/ Binder**	**Water/ Binder**
50%	20%	10%	20%	0.2	3

The aimed dry densities to be obtained for the specimens are 157 [kg/m²] and 320 [kg/m²] for HH and LH, respectively [29]. The total porosity of the studied hemp/lime mixtures ranges from 45 [%] for LH to 62 [%] for HH [25]. The porosity of hemp/lime mixtures includes a variety of pores, from micrometric pores in binder and hemp shiv to millimetric pores between hemp shiv and binder [19]. Due to the difference in hemp/binder ratio, there will be more millimetric pores in HH which gives the higher porosity.

Thermal Properties

Thermal conductivity for HH and LH is 0.057 [W/m*K] and 0.112 [W/m*K] at dry density, respectively. The specific heat capacity is 470 [J/kg*K] for LH and 400 [J/kg*K] for HH. The result underlines with [13], which studied an increase of density will increase thermal conductivity. Furthermore, binder with more hydraulic content will increase thermal conductivity and specific heat capacity [14], which corresponds with the result of HH and LH.

Hygric Properties

Sorption isotherms and moisture permeability [25] [29] have been tested. The sorption isotherms show good properties for moisture uptake and moisture release. HH properties as a moisture regulator are greater compared to LH.

Diffusion coefficient tested by ODA equipment show that increased hemp-shive to binder ratios increases diffusivity. Results from ODA do not under line with [34], where two types of hempcrete mix with different hemp shive to binder ratios have similar diffusion properties at low humidifies (<95 [%]).

Table 2 - Hempcrete material properties

Parameter	High Hemp	Low Hemp
Density	157 [kg/m³]	312 [kg/m³]
Thermal conductivity	0.06 [W/m*K]	0.114 [W/m*K]
Specific heat capacity	400 [J/kg*K]	470 [J/kg*K]

High Hemp		Moisture content	
	RH	**Adsorption**	**Desorption**
Sorption isotherms	0	-	-
	18	3.22	6.93
	34	4.83	8.41
	54	7.4	10.35
	80	12.96	-

WVP gas		
RH	**HH**	**LH**
0%	5.2E-9	5.6E-9
44%	1.9E-8	1.9E-8
60%	2.0E-8	2.2E-8
80%	3.7E-8	4.6E-8

2. Skamol

Composition and manufacturing

Calcium silicate (CaSi) - main two ingredients creating the CaSi board is micro silica (side product from ferrosilicon and silicon metal production), and quicklime (calcination of limestone). Production of the material is divided in two steps. During first one all the chemical reactions take place, while second is focused on conditioning and shaping the material. There are other calcium silicate products from the company, however that particular one (Living Board) presents highest moisture buffering abilities and is recommended for tackling high humidity problems indoors [22].

SkamoInnerwall – (Moler brick) presented as diatomite / clay bricks is in fact moler mixture. The raw material extracted from island Fur (Denmark) is a diatomite form of 55-70 [%] diatoms (silica frustules from prehistoric algae) and 30-45 [%] clay minerals. Delicate layout of diatomite with multiple micropores (below 1 micrometre) provides great insulation abilities. Mixed additionally with fired off fine grained wooden saw dust, leaves additional cavities lowering thermal conductivity while high content of iron results in needed strength.

Material properties

CaSi - boards are capillary active being able to transport moisture from cold to warm side of the wall. The product was tested in lab conditions in terms of fungal growth on their surface with conditions 28 +/- 2 [°C] and RH of 95 +/- 4 [%] for 7 weeks. Results showed that the material prevents fungi growth on the surface when they are exposed to presented temperature range and high moisture content. Mould was however observed in comparable materials – pine sapwood and gypsum boards [35].

SkamoInnerwall - Material can be used only for inside construction, as exposed to weather conditions are destroyed - when outside temperature goes below 0 [°C], the accumulated water freezes and breaks the bricks. Paper [36] shows that 380-580 kWh annually can be saved on heating while using Moler brick instead of usual one (with applied insulating mortar).

Both materials are produced in standardized manner with set recipes (commercial products), hence are expected to have very similar properties as in available datasheets. However, some of the parameters will be validated. Larger amount of data is present for CaSi boards.

Thermal Properties

Thermal properties for both materials are presented in Table 3 below. It is worth to mention that specific heat capacity of Moler brick is estimated and not derived experimentally.

Hygric Properties

Hygric properties were only measured for CaSi board and results in great sorption ability (Table 3).

Rest of the properties can be seen in Appendix B along with detailed description of the products.

Table 3 – Skamol materials properties

Parameter	CaSi	Moler Brick
Density	220 kg/m³	700 kg/m³
Thermal conductivity	0.054 W/m*K	0.15 W/m*K
Cp	840 J/kg*K	800 J/kg*K
WV diffusion resistance (μ)	3.5	-

CaSi moisture content	
RH [-]	**Sorption**
0.3	8.92
0.65	14.1
0.8	20.37
0.93	38.43
0.97	59.69

3. Performed measurements

Some parameters of selected materials are already measured by various research paper. Although materials differ in terms of density, mixing ratio and used components (for hempcrete material), already performed tests could act as reference data. Based on selected measurements in the paper, following values are already derived presented on Table 4:

Table 4 - Already performed measurements

	HH	LH	CaSi	Moler brick
Thermal conductivity	x	x	x	x
Specific heat capacity	x	x	x	-
Moisture sorption	x	x	x	-
Moisture permeability (Cup)	-	-	x	-
Moisture permeability (ODA20)	x	x	-	-

4. Renders

The following paper will investigate renders effect on moisture permeability. Three different renders, LH, SkamoWall Smooth plaster from Skamol company (SSP) and DuraPuds 710 from Alfix company will be applied on 3 samples for each base material - high-hempcrete, CaSi and moler brick.

LH is described in Section A.1 were also material properties are presented. Both SSP and DP are commercially available plasters which are cement based and considered breathable due to diffusion open structure. Their properties are presented in Table 5. SSP is developed for surface finish on CaSi and moler brick walls. DP is commonly used as plaster on concrete and brick.

The renders will be applied with thickness of around 10 [mm] on 3 mentioned materials and measured by ODA20 equipment. Results will be compared with the one obtained via materials without applied render and hence their vapor permeability will be analysed.

Table 5 - Properties of DuraPuds and SmoothPlaster

Material	Density [kg/m³]	WV Diffusion Resistance [μ]	Absorption of Water [Class]
SSP	1400	≤ 15	W0
DP	1400	≤ 25	W2

B. Methods

Following section will present the type of measurement and used equipment. The properties are divided into thermal and hygric ones.

Thermal properties

1. **Thermal diffusivity (α) and specific heat capacity (Cp)** – LFA 447 equipment

Thermal diffusivity [mm²/s] is a thermal inertia of a material (momentum of heat transfer through the sample - from the hot to the cold side). LFA 447 by Netzsch Geratebau GmbH equipment (Laser flash) is used where **α** of the material is determined by laser shots warming up the sample on one side. The opposite side records temperature versus time change. Considering heat transfer analysis, the parameter can be described as presented in Equation 1:

$$\alpha = \frac{\lambda}{(\rho * C_p)}$$

Equation 1 - Deriving thermal diffusivity with Cp, density, and thermal conductivity

Hence, determining the specific heat capacity can be done by knowing the thermal conductivity, density and obtained thermal diffusivity.

Cp [J/kg*K] presents required quantity of heat energy for a material added to the mass, to rise its temperature. Same equipment as for thermal diffusivity is used, where initially by obtaining thermal diffusivity, specific heat capacity is derived.

Comparative method is applied for the measurement – test and reference sample (with already known parameters, possibly similar to the test sample) are exposed to same test conditions. Analysing both samples maximum temperature and related parameters, Cp of test sample is measured by Equation 2:

$$c_p^{test} = \left(\frac{T_{max}^{ref}}{T_{max}^{test}}\right) * \frac{q * l^{ref}}{q * l^{test}}$$

Equation 2 - Deriving Cp with equipment parameters

*Where T_{max} is maximum temp of the sample [°C], q is the density [kg/m³] and c_p^{ref} is reference sample specific heat capacity [J/kg*K].*

The calculation method used by LFA 447 is limited to near adiabatic conditions which is obtained by high thermal diffusivity samples with small thicknesses and short measurement time. Samples with lower thermal diffusivity has longer measurement time, and thus heat loss from convection and radiation cannot be ignored. If adiabatic conditions are not present, recalculation models have been developed to take this into account.

The purpose of conducting the measurement is to retrieve input data for dynamic simulation and compare values with obtained one by the company and previous tests.

The samples of this study are prepared with diameter of 12.7 [mm] and thickness of Moler brick and CaSi of 2.03/2.6 and 4.8 [mm] respectively. CaSi samples are moulded directly into the frames since it was not possible to cut a solid material, as of the Moler brick.

It is important the samples have an even surface and thickness to get uniform heat transfer through the solid. Samples are coated with thin graphite layer just before measurements to increase temperature responds on the surface. There is no other need of conditioning the samples beforehand. Detailed description of apparatus can be seen in Appendix C

<u>Hygric properties</u>

1. **Sorption isotherms** – VSA equipment

Moisture sorption isotherms illustrates mass change of investigated material, during water activity being adsorbed or desorbed by the material at constant pressure. There are two known ways to measure sorption isotherms, continuous and discontinuous method [37] [38]. The continuous method conducts sorption curves under quasi-equilibrium conditions. The adsorptive is admitted at a slow and constant rate. Volumetric or gravimetric techniques is used to measure the variation of water increase or decrease by measuring the variation of pressure. The discontinuous method conducts sorption isotherms by varying vapor concentration surrounding the adsorbent and measure the change in mass at different stages. Both methods can be performed by VSA equipment. The DVS has been created to shorten the measurement time on small samples.

In this study, the sorption isotherms are conducted accordingly to the VSA equipment, where DDI method (dynamic dew point isotherms - continuous method) is used. The moisture content is established by simple Equation 3 presented below:

$$m\% = \frac{(m_x - m_0)}{m_0}$$

Equation 3 - Calculation of moisture content by mass increase

Where, Mx is mass at specific relative humidity [kg] and M0 is dry weight mass [kg].

Measurement is concluded in RH range of 10 to 90 [%], while the build-in scale is weighting the sample at various RH level. Dry weight is obtained afterwards by drying the material in oven with 105 [°C] to calculate the moisture content at each derived point. More than a few cycles are required to obtain reliable data and ensure isotherms are repetitive. According to [38] VSA equipment, the weight of the sample needs to be within range of 500-5000 [mg] and specific shape is not specified. Due to small sample size, the measurement time is short allowing to obtain an isotherm in around 1 day. Description of apparatus can be seen in Appendix D

2. **Moisture permeability**

Moisture permeability measurement is done by two methods, traditional Wet Cup / Dry Cup-Method (Fick's first law - moisture diffusivity) and by recently presented for building materials fast-results-orientated ODA20 equipment.

a. Climate chamber – Dry Cup method

Traditional method for assessing the water vapor permeability (δ_v [kg/m*s*Pa]) under isothermal conditions presents ability of water vapor to transfer through specimen under steam flow pressure. Samples are prepared (cut & moulded), conditioned (23 [°C] and 50 [%] RH to reach equilibrium) in climate chamber and tested with aqueous solution (salt with 0 [%] RH) and weighted at selected time intervals, as according to ISO12572:2016 [26]. The measurement time depends on the sample and can take from few days to a few months. Calculation is performed according to Chapter 8 [26] where water vapor resistance factor is the outcome of calculation method, as on Equation 4:

$$\delta_v = \frac{G * e}{\Delta P_v * A}$$

Equation 4 - Calculation of water vapor resistance factor

Where, G is the mass rate [kg/s], e is sample thickness [m], ΔP_v *is the vapor pressure gradient [Pa] and A is the surface area [m2].*

Method is time-consuming and hence applied only for CaSi and HH to, along with ODA20, obtain the retardation factor. Sides are sealed (wax and paraffin or PVC) to allow one-way transfer. Same mixture was applied to seal samples to the cup, as presented on pictures in Appendix E. Measurement provides with effective diffusivity, while ODA20 with the independent diffusivity.

b. Oxygen Diffusion Apparatus 2020 (ODA)

Method often utilized in soil physics research field, however just lately introduced for building materials to investigate their moisture transport [29]. Nitrogen is flushed into closed chamber below sample to remove the oxygen. Oxygen from surroundings is then diffusing via the specific specimen into the chamber until the level of ambient air is reached. Due to forced flow, water vapor diffusivity differs from traditional method – parameters as surface diffusivity, sorption and capillary condensation are disregarded. Measurement time estimated at 1-3 hours presents large upgrade from conventional method. Obtained diffusion coefficient [cm^2/s] from measurement needs to be transformed to relative gas diffusivity to calculate water vapor diffusion, as presented on Equation 5:

$$Dp_{H2O} = (Dp_{O2}/Do_{O2}) * Do_{H2O}$$
$$\delta_p = (Dp_{H2O} * \rho * \frac{\Delta u}{\Delta\varphi})/P_s$$
Equation 5 - Calculating WVT from ODA20

Measurement is concluded on all presented materials, where LH is validated only (hence only 2 samples). 9 samples of HH, CaSi and Moler brick are tested as it provides greater certainty in the result as poor-quality samples can be more easily identified and omitted. Followingly, the samples are re-used and coated with render. Measurement is conducted in the lab environmental conditions, registered by the sensor. The samples are conditioned in the room before measurement to reach equilibrium and system description is in Appendix F

c. Retardation factor

Retardation factor is developed to obtain the effective water vapor permeability from the measurement conducted by ODA20 equipment. As stated in [29] the new method results in larger effective diffusion, presenting gas diffusivity as independent effusivity. Retardation factor covers the processes existing in water vapor diffusivity of standard Cup Method, not present in gas diffusivity (surface diffusion, sorption, capillary condensation, and effusion). [29] Factor, *R*, derived from first measurement is also calculated in following paper to indicate, whether other material type will result in same or completely different factor.

3. Moisture buffer value

The ability to influence moisture variations in the room by building materials can be shown as their moisture buffer performance. That property is presented by hygric materials, interfering with surrounding space to reach equilibrium with RH by ad-/desorbing moisture peaks. NORDtest protocol is most frequently used in Europe, determining moisture buffer capacity in theoretical and practical way [11].

Theoretical Moisture Buffer Value – moisture effusivity

Moisture effusivity (b) is determined based on already obtained material parameters and the principle lies as for the analogy of heat & mass transfer. By using that analogy, the thermal effusivity used for heat transfer is converted to moisture effusivity, *b* [kg/(m^2*Pa*s$^{1/2}$)] [11] [39], for materials capabilities to take in and release moisture (moisture intake rate) when the surface is exposed to humidity variations, calculated as on Equation 6:

$$b = \sqrt{\frac{\left(\delta_p * \rho_0 * \left(\frac{\Delta u}{\Delta\varphi}\right)\right)}{p_s}}$$
Equation 6 - Calculation to obtain moisture effusivity

*Where δ_p is water vapor permeability [kg/(m*Pa*s)], ρ_0 is dry density [kg/m^3], u is moisture content [kg/kg], φ is relative humidity [-] and p_s is saturation vapor pressure (from test conditions) [Pa].*

Theoretical Moisture Buffer Value - Ideal

The ideal MBV is the theoretical approach to obtain the value, as the amount of water intake / release during moderation of RH on the surface is similar to the conditions in practical MBV approach but with moisture effusivity, hence steady-state error. MBV_{ideal} is approximation of real MBV, as ideal experimental condition seldom occurs, hence can be presented as material characterization [40]. Assumption considers also thickness of specimens, equal or above their penetration depth. MBV_{ideal} (calculated with Equation 7) is dependent on time period, saturation vapor pressure and moisture effusivity. Of interest is time dependent, repeating signal pattern with high and low levels of humidifies – 8 hours of 75 [%] RH (moisture uptake) and 16 hours of 33 [%] RH (moisture release).

$$MBV_{ideal} \approx 0.00568 * P_s * b\sqrt{\tau}$$
Equation 7 - Calculation to obtain MBVideal

Practical Moisture Buffer Value

Practical approach to MBV is done via experiments where actual MBV is determined. Measurement time should correspond to usual variations in real-life (normally daily changes) materials coatings and thickness. $MBV_{practical}$ [g/(m^2%RH)] is determined as amount of moisture that is transferred via open surface of investigated material while exposed to variations in RH. Calculation can be seen on Equation 8:

$$MBV_{practical} = \frac{\Delta m}{A * (RH_{high} - RH_{low})}$$
Equation 8 - Calculation to obtain MBVpractical from measurement

Where, Δm is moisture intake and release [g], A is open surface area [m^2] and $RH_{high/low}$ is high/low RH level [%].
Samples need to be created, conditioned in climate chamber and tested, as according to [31].

Moisture penetration depth

Penetration depth, $d_{p1\%}$ [m] is a thickness of the tested material, where moisture content variations are still present at the surface, and can be recorded, but are almost completely damped. Material thickness needs to be equal to $d_{p1\%}$, or larger, in order to obtain meaningful outcome of the whole MBV, otherwise the buffering abilities are not present to that extent. Equation 9 provides with depth where the amplitude is up to 1 [%] of the surface variation in selected time period [s].

$$d_{p1\%} = 4{,}61 * \sqrt{\frac{D_w * t_p}{\pi}}$$

Equation 9 - Calculation to obtain penetration depth (mm)

Where D_w [m^2/s] is moisture diffusivity presented on Equation 10:

$$D_w = \frac{(\sigma_p * p_s)}{\rho * \frac{\Delta u}{\Delta \varphi}}$$

Equation 10 - Calculation to obtain moisture diffusivity

Moisture buffer classes

Once the MBV is obtained, the material can be put on the MBV classification scale and be compared to other building materials. There are in total five levels ranging from negligible to excellent, as presented on Figure 1 below:

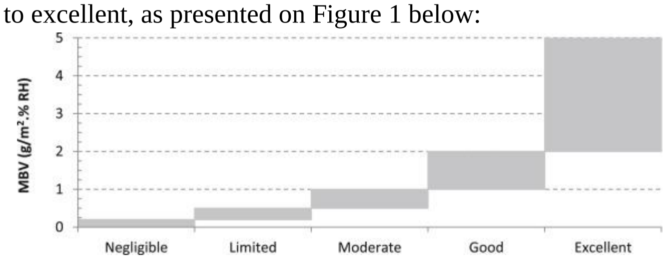

Figure 1 - Classification of MBV [11]

C. BSim – dynamic software

Dynamic building simulation software to compute integrated and measured data will be used for investigation of indoor climate with highest focus on transient moisture content. BSim program is able to simulate, among other factors, possibly to indicate difference while using hygric materials to passively regulate RH.

a. ***Model***

Following model is represented by single room with rectangular layout and one window pointing towards north. Only one wall is exposed to the outdoor conditions, while the rest (3) are internal walls exposed to same thermal zone. Several separate models are made with same heat and moisture loads (internal gains), ventilation rate, heating and even infiltration, but different construction on the external wall. The materials are: (1) EPS, (2) Lightweight concrete (LC), (3) Hempcrete, (4 & 5) Skamol CaSi on LC and brick construction, (6 & 7) Skamol Moler brick on LC and also brick construction. Each room has 16 m2 of floor area and 40 m3 of volume. Detailed construction layout of the created walls can be seen in Appendix G. Nevertheless, all constructions are currently used in practice for single-family houses with airtight construction and are better than maximum from Building Regulation 2018 [41].

All the other surfaces, besides external wall, are covered with dampproof layer to account for moisture buffering properties of the investigated wall only. External wall is selected instead of internal to evaluate the operation with outdoor conditions.

b. *Simplification for simulation*

It is decided to perform simulation on 1 room only to minimize the complexity of the model and focus on moisture buffering abilities of the materials, instead of various examples with geometry or adjusting systems to better fit the envelope, but still account for real-life scenario data (loads and different constructions).

c. Moisture and heat loads

User behaviour, occupancy rate and appliance schedules are based on [42] to present normalized rate of loads in apartment / domestic building. The standard for which the measurement was done is currently EN 16798-1:2019.

Heat and moisture generation from human body is based on [43] rather than on [42], as the first one focuses purely on the human factor. It is decided to account for one occupant, as the space is small enough to represent one's bedroom or home-office.

d. Systems

Ventilation is set to be fixed (CAV) with 0.5 [ACH] – low rate is selected to inspect more thoroughly the materials buffering abilities in high humidifies, however larger ACH (1 & 2 [h^{-1}]) is also studied to account for RH amplitude with increased ACH.

Constant ACH is achievable by the Return Air control and system is running whole year.

Convective heating (radiators) is used with setpoint of room thermostat of 22 [°C] operative temperature, as mean value of category B in heating season from ISO15251:2007.

Infiltration rate is taken from [44] while investigating the PUR detached house with as well airtight construction and hence is set for all the models with fixed rate of q50=0.066 [l/s/m^2].

Weather data is based on DRY Danmark_2013 transcript with building location in Copenhagen, Denmark (as default), with open flat country terrain.

Detailed systems input with load parameters and control is presented in Appendix G.

III. Results & Discussion

Results section is divided into separate outcomes from measurements, simulations and calculations, while short discussion follows each sub-section.

A. Results from measurements

1. Thermal diffusivity and Specific heat capacity

Both products from Skamol company were measured by laser flash equipment at 4 different temperatures. 10 shots were applied for each temperature and mean value of each of them was calculated. Due to composition of hempcrete material and required size and shape of the specimen, the measurement failed at withdrawing the outcomes.

Presented below are Figure 2 and Figure 3 with Cp and thermal diffusivity, as well as Table 6 with mean value for BSim input.

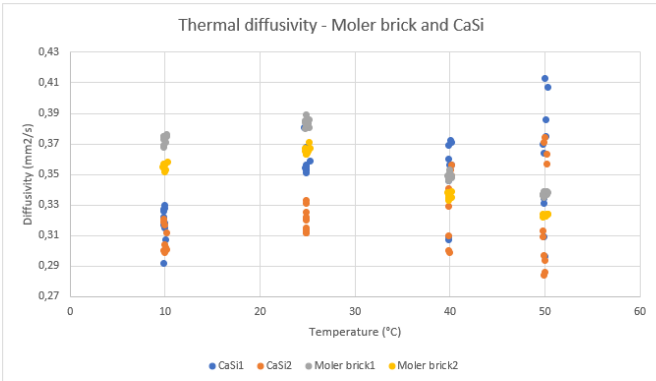

Figure 2 - Moler brick and CaSi thermal diffusivity

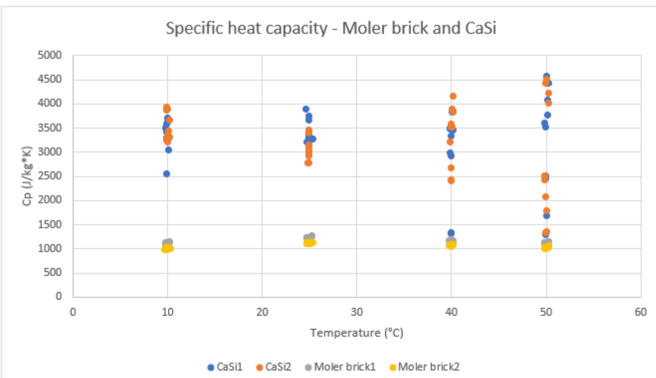

Figure 3 - Moler Brick and CaSi specific heat capacity

Table 6 - Cp and thermal diffusivity of Skamol products

	Thermal Diffusivity [mm²/s]	Specific Heat Capacity [J/kg*K]
CaSi	0.33	3220
Moler Brick	0.35	1160

CaSi results presents a mean thermal diffusivity of 0.33 [mm²/s]. The parameter has not been tested by Skamol, hence it cannot be compared and the result cannot be validated.

There is an enormous difference in measured specific heat capacity compared to initially provided parameters from the company. The mean specific heat capacity is 3220 [J/kg*K] which is around 4 times larger than measured and stated by the company on 840 [J/kg*K] (Table 3). The deviations are large within the samples, especially at high temperatures and reason of these results is likely related to quality of the samples, as due to required small sizes their surface lacked smoothness (crucial for the measurement). Another reason can be connected to the fact of moulding material directly into specimen frame, destroying the structure and composition despite achieving same density.

Moler brick outcomes are steady and the temperature curve fits the reference model. Thermal diffusivity is 0.35 [mm²/s] with a standard deviation of 0.002. The specific heat capacity is measured to 1160 [J/kg*K] which is higher than estimated by the company (800 [J/kg*K]) but was never calculated. These results from the measurement on LFA 447 is considered valid, due to a low standard deviation and a minimal discrepancy of 104 [J/kg*K] between the mean values of the two samples.

Moler brick results will be used in dynamic simulation and full calculation is presented in Appendix C.

2. Sorption isotherms

Moisture sorption and desorption is determined by the VSA equipment described in Section 1 and Appendix D. Eight isotherms are derived for Skamol materials, while only four were determined of the HH and LH. Presented on Figure 4 are isotherms of all materials together, while separate isotherms for all cycles are presented in Appendix D. The values are used in further simulation in BSim software.

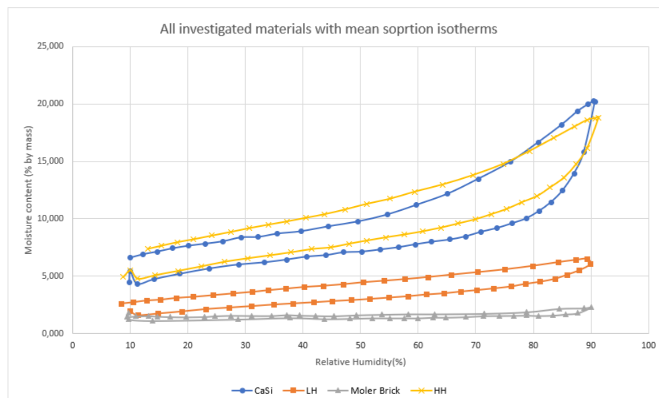

Figure 4 - Isotherms of analyzed materials

As expected, the results from Moler brick does not appear in smooth ad- and desorption curves but follows traditional brick, more unpredicted path and does not have great moisture abilities. They are however larger than from comparable literature [45] [46] but for instance lower than calcium brick [47]. CaSi board presents steady increase and decrease in moisture content at various humidifies as well as are hempcrete materials. The silicate board results in great water sorption abilities compared to [46], however compared to the data from company, the board indicates a bit lower performance during test concluded by VSA (Figure 5). That could be related to size and quality of the sample, as well as measurement method which might better register changes in higher humidifies.

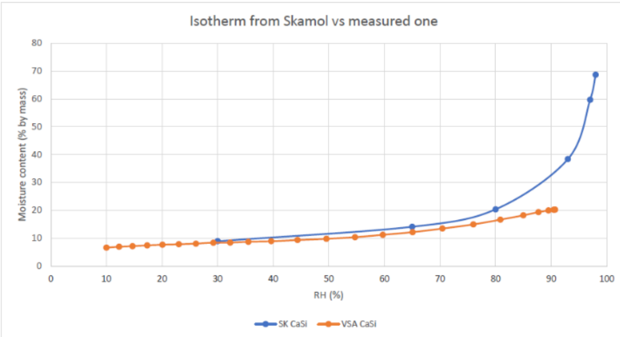

Figure 5 - Comparison of CaSi isotherms

The CaSi accounts for higher water absorption in greater RH than HH, however lower midway humidifies. It is not suspected, as it was presumed that HH will have highest moisture sorption abilities. LH with larger hemp shiv to binder ratio than HH falls below the CaSi and HH materials, and is highly comparable to [25], although the densities vary (560 vs 360 [kg/m^3]). The HH although has similar density to [29] the analysed material presents better moisture sorption abilities. The measurements confirm that high porosity materials are accounted for storing larger moisture content.

Appendix G presents the input data of each material insert to dynamic simulation.

3. Moisture permeability

Water vapor transmission is retrieved via two methods, while the traditional one is utilized for CaSi board and HH only at 23 [°C] and 50 [%] RH. The new, rapid method (ODA20) was conducted on all investigated materials including plasters. The measurement was performed at average of 23.4 [°C] and 34 [%] RH (Appendix H – datasheet from IC meter) corresponding to small lab environment at AAU building on the 5th floor.

a. Cup method

Water vapor permeability is calculated based on mass change after the samples themselves has reached steady state conditions. Steady state is reached when 3 measurements in a row have mass change variation of maximum 5 [%]. The hempcrete experiment was stopped before specimens were within required range. Therefore, there are large variations in the results, especially sample 2 and sample 4 have large variations of the water gain compared to the other samples. Therefore, only the outcomes from specimens 1, 3 and 5 are used in the results as they correspond to 5 [%] variations. During the measurement the salt solution placed below sample is sealed and moisture is penetrating only through the specimen, hence whole set is increasing weight until it stabilizes. Presented below on Figure 6 is mass change of 5 CaSi specimens with registered time reaching equilibrium.

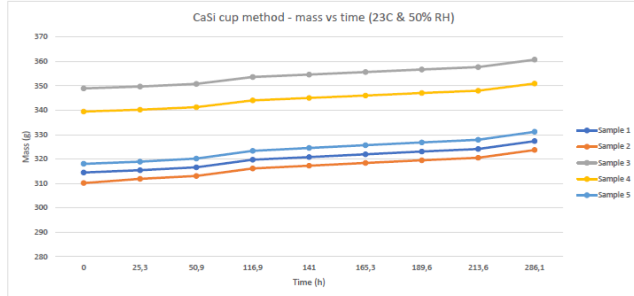

Figure 6 - Mass change of CaSi sets

Measurement of HH high-hempcrete resulted in water vapor transmission (WVT) of 4.84 * 10^{-11} [kg/m*s*Pa]. It was not presumed, as based on literature the value was suspected to be higher, due to low density and large hemp shiv ratio [18].

WVT of CaSi board resulted in 4.93 10^{-11} [kg/m*s*Pa] being 11.4% lower than the producer provides, which can be related to the quality of obtained materials and quality of prepared samples, as same equipment was used. Worse value decreases moisture effusivity, increase penetration depth and affect MBV in general, as water vapor transmission is present in all mentioned parameters.

Results indicate slightly better moisture permeability of CaSi board than HH, indicating better hygric property. Detailed calculation is presented in Appendix E.

b. ODA20

Diffusion coefficient from ODA20 equipment is acquired via script retrieving the value based on sample height and time required for chamber to be in equilibrium with surrounding. The results of investigated materials are presented on Figure 7 and Figure 8:

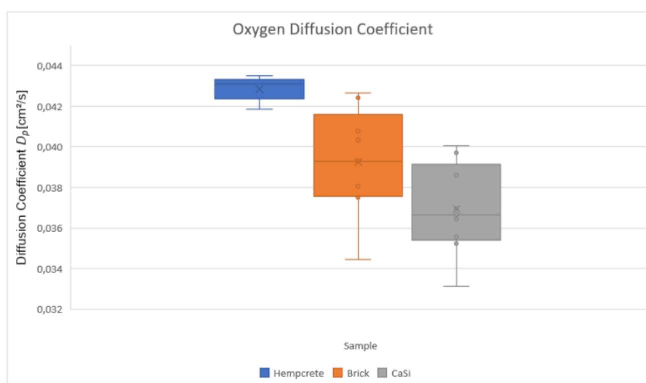

Figure 7 - Diffusion coefficient of the materials as a function of moisture content

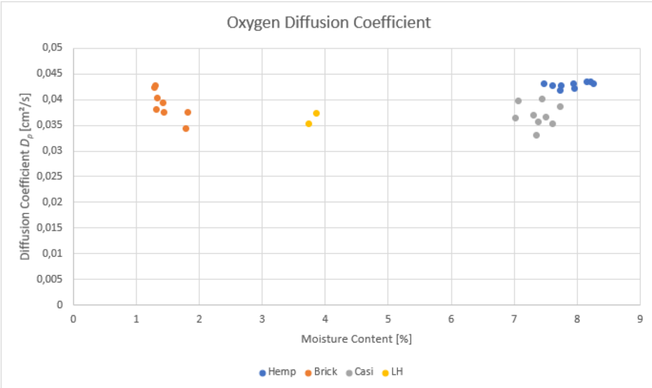

Figure 8 – Diffusion coefficient dispersion at 35 [%] RH

The results show that hempcrete is the most vapor permeable with a mean value of 0.0428 [cm²/s] at a moisture content of 7.9%, where Moler brick and CaSi have a mean value of 0.0039 [cm²/s] at a moisture content of 7.37% and 0.0037 [cm^2/s] at a moisture content of 1.45%, respectively. The two tested LH samples are comparable to the previous tested LH samples by AAU, with a mean value of 0.036 [cm²/s] with a moisture content of 3.82%. HH and LH samples for this study has a higher density of 176 and 366 [J/kg*K] respectively, compared to 156 and 312 [J/kg*K] [29]. The different density did only influence the HH result, where compared to previous test (AAU – 0.0455 [cm²/s]) measured sample has a lower value at the same moisture content.

The results from hempcrete are considered more reliable than from Skamol product, as the amplitude of obtained value is 0.0016 [mm²/s] which is a small deviation compared to the CaSi and Moler brick, which have an amplitude of 0.0069 and 0.0082 [mm²/s] respectively.

The reason for the small deviation in the hempcrete results is related to casting the samples directly into the cylinder, which does not cause air pockets between the material and the cylinder, where oxygen can penetrate more easily. CaSi and brick are, as mentioned in Section 5, sealed to the cylinders with a mixture of paraffin and wax, creating filling empty spaces with the sealant. Twice the amount of wax was on average applied on the CaSi samples compared to Moler brick samples due to a minor diameter of drill, which can be the reason of CaSi results has a smaller deviation. It is observed that some of the samples do not have wax in the entire cavity (as they were pressed into the cylinders) which will allow air to travel out into the cavity and affect the result in a positively way by resulting in larger moisture diffusion.

From the Equation 10, following outcome is calculated for investigated materials presented on Figure 9 below:

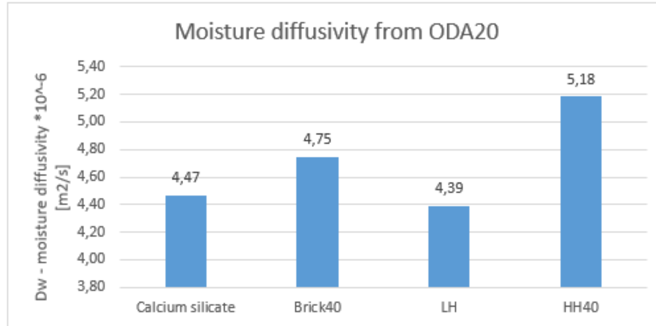

Figure 9 - Moisture diffusivity of analyzed materials

Moisture diffusivity is proportional to WVT, hence surprisingly in following outcome the HH has better diffusion parameter than CaSi (compared to Cup Method). As not suspected, the Moler brick presents higher moisture diffusivity than CaSi. Differences may be caused due to applied casting and cutting method. Comparison of ODA20 and Cup method WVT of both materials is presented along with retardation factor on Table 7, in Retardation factor section.

As mentioned in Section 4, 3 renders were applied on CaSi, Moler brick and HH. The Diffusion coefficient of base materials with renders and the impact in percentage to the base material are presented in Appendix F. Figure 10 illustrates the impact of applying renders on HH samples.

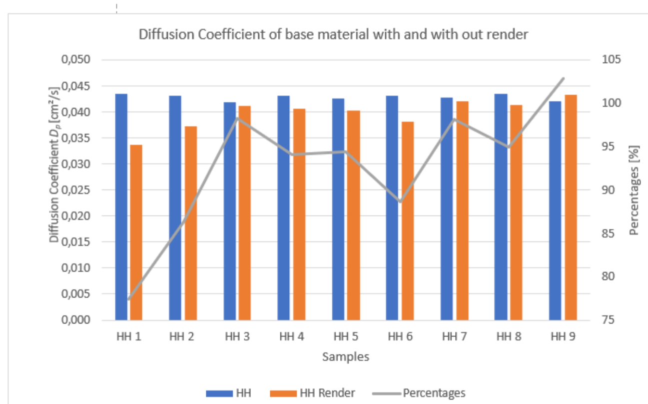

Figure 10 - Renders applied on 9 HH samples

Application of LH, SmoothPlaster and DuraPuds on HH reduces the parameter to 98.65, 92.38 and 87.32 [%] respectively.

It is observed that investigated plasters are reducing moisture diffusivity of the material used as internal cladding despite some plasters might have similar diffusion, as seen on CaSi, where LH is applied which has a similar diffusion coefficient, but the result is lower (Appendix F).

Due to large variation on how the render influenced the diffusion coefficient, further tests are needed to determine the impact of the applied render.

B. Retardation factor

While comparing two identical samples measured with different method, the factor is in fact just a difference between them as units remains unchanged.

Although environment of the Cup Method differs slightly from ODA20 (RH is around 15 [%] lower in ODA20), the measurement of WVT is not straightforwardly influenced by RH, but by moisture content (MC). MC is managed in the calculation of moisture diffusion (from sorption isotherms), however correlation of ambient RH to measurement outcome was noticed in ODA20 equipment. Due to capillary condensation, pores filled with water restrict the transport in larger ambient humidifies, narrowing the air passage [18].

For analysed material, following retardation factor is derived presented in Table 7:

Table 7 - Calculated retardation factor of analysed materials

	CaSi	HH
WVT Cup method [kg/m*Pa*s)]	4.93E-11	4.84E-11
WVT ODA20 [kg/m*Pa*s)]	5.46E-08	5.68E-08
Retardation factor [-]	1106	1173

Values are compared with [29], where retardation factor varies from 200 to 800 with an average of 360. Obtained value for hempcrete material is exceeding the range of retardation factor from the reference source. CaSi material results also in large difference between two measurement types. Outcomes indicates that more measurements should be concluded, also on various initial RH of the samples. Conclusion from paper [29] presents that with larger RH, larger is the retardation factor while obtained HH factor of 1173 is almost three times larger (413) than for comparable RH from the paper.

C. Moisture buffer value

a. Moisture effusivity

Calculation of moisture effusivity is required to further obtain MBV_{ideal} and penetration depth, therefore only the materials which were tested via Cup Method can have obtained values. Detailed calculations are present in Appendix I and presented below is the result with reference samples from literatures:

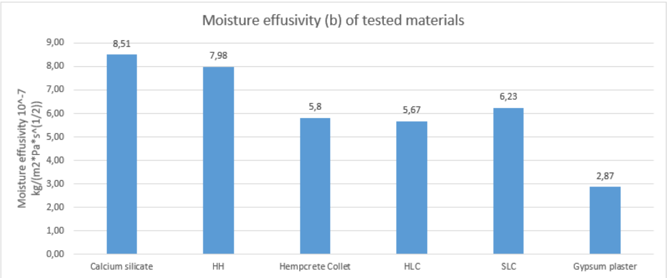

Figure 11 - Moisture effusivity [21] [48] [49]

b. Ideal MBV and moisture penetration depth

The MBV_{ideal} and true moisture penetration depth is derived for calcium silicate and HH, using the method presented in Section 6. Due to the range of RH in $MBV_{practical}$ (33-75 [%]), the ∂u is selected as mean from ad- and desorption isotherms. Calculated MBV_{ideal} with comparable materials from literature is presented on Figure 12, while penetration depth with also literature references is on Figure 13:

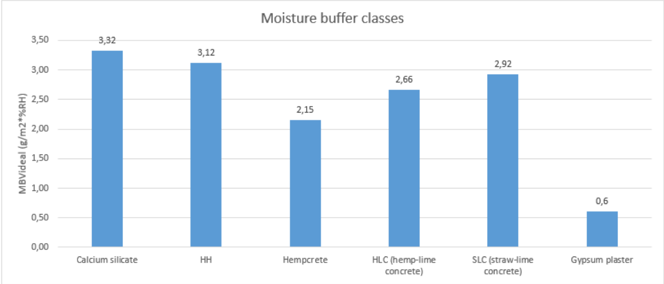

Figure 12 - MBV_{ideal} of tested and reference samples [21] [48] [50]

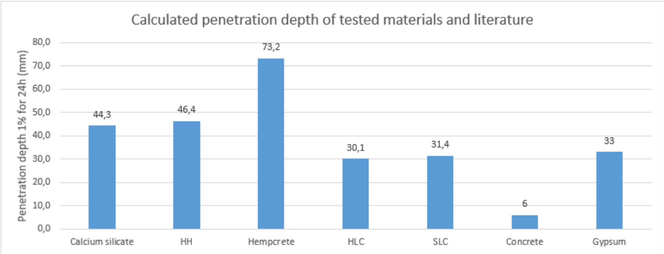

Figure 13 - Pd of tested and reference samples [21] [48] [49]

Based on the MBV_{ideal} values, both analysed materials are having excellent properties on MBV classification scale and have in fact similar values, which is also confirmed by moisture effusivity and WVT from Cup Method and ODA20. The result would need to however be confronted with $MBV_{practical}$, as practical approach is more realistic. MBV_{ideal} is higher for CaSi than HH.

Based on literature its noticed that analysed HH has higher moisture effusivity and better MBV_{ideal} along with lower penetration depth to compared literature, which was assumed. Applying gypsum board on the wall reduces hygric performance of the building, as presented on figures above.

c. Practical Moisture Buffer Value

With the possibility of performing $MBV_{practical}$ according to NORDtest protocol, the outcome could not only be compared to literature but also to MBV_{ideal} to account for reliability of MBV_{ideal} for classification and hence validate precision of undertook tests. Moreover, the graph obtained during mass change of the material would be compared with simulated in BSim software period with and without moisture generation. Although the values with high probability would differ, the patterns could be analysed against each other. With retardation factor from ODA20, the MBV could be calculated by use of VSA and ODA20 equipment only while knowing the materials density. Comparable MBV_{ideal} and $MBV_{practical}$ would state as proof, that Cup Method and $MBV_{practical}$ is not further needed for material scale tests to obtain MBV, lowering drastically the measurement time.

D. Results from dynamic simulation – BSim and indoor environment

Simulation in dynamic software is performed to account for moisture buffering abilities of hygric building materials. Several construction variations are created to comprehend the difference between them. It is found out that under same input parameters the yearly RH with hygric construction is lower not only in peak periods, but also by obtaining numerical mean, as presented on Figure 14. Operative temperatures on the other hand are in larger percentage in 4^{th} category (DS15251:2007) (Figure 15), especially in summer period (Figure 16). Construction with hempcrete has most desirable indoor relative humidity, followed by CaSi applied in lightweight concrete construction, CaSi applied on brick construction and Moler brick applied also on brick construction.

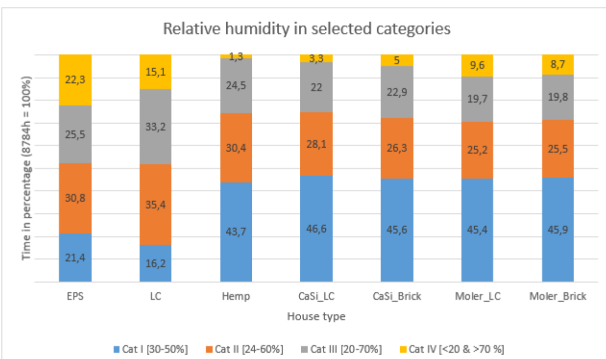

Figure 14 - Simulated RH over a year according to DS15251:2007

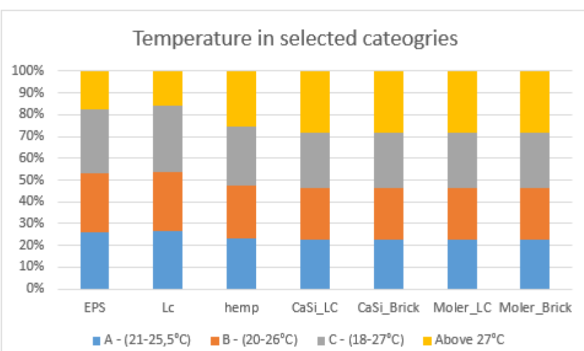

Figure 15 - Operative temperature over a year (DS15251:2007)

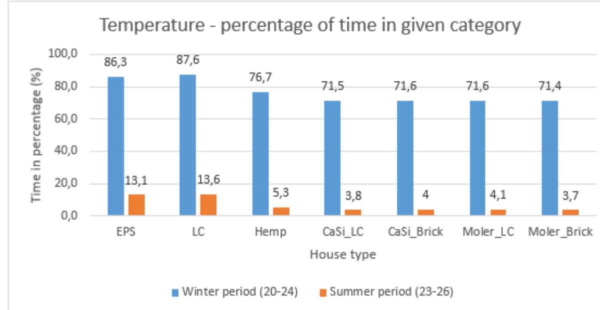

Figure 16 – Percent of time in summer and winter period (T_{op})

As warmer air has ability to possess more moisture, the humidity can genuinely vary, as one solution to decrease indoor RH is to increase temperature. Hence, the least moisture-permeable construction (EPS) is compared with the most one (hempcrete) for the day with highest RH in EPS house (Figure 17).

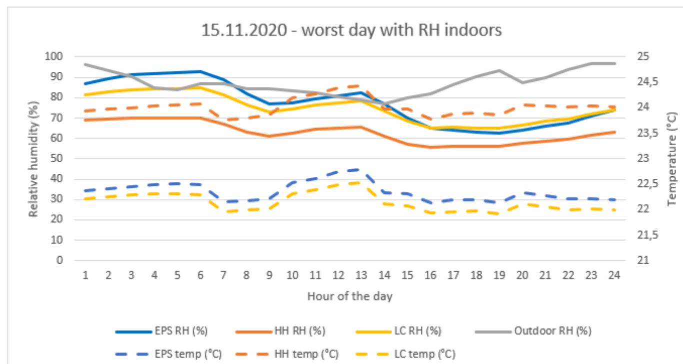

Figure 17 - Difference between RH and Top between houses

The graph presents that the operative temperature in hempcrete house in on average 1.5 – 2 [°C] higher during the day with 6-22 [%] lower RH. To account for moisture abilities, the moisture content [g/kg] is obtained from IX diagram for 2^{nd} hour of the day (as an example) with 1.5 [°C] and 20 [%] RH difference. Conditions in EPS house results in 15 [g/kg] of moisture content in dry air, while in hempcrete house the value is 13 [g/kg]. Multiplying the difference with dry air density (1.205 [kg/m^3]) and volume of the room (40 [m^3]), the total difference equals to 96.4 [g] of moisture absorbed by hempcrete wall. Although the temperature is higher, the moisture content is lower as it is being absorbed by hemp wall.

Distribution of yearly relative humidity inside the investigated constructions is presented on Figure 18 along with humidity ratio [kg/kg] indoors. Figure presents that although the RH varies between investigated cases (especially around March and November months) the indoor moisture content has much lower discrepancy.

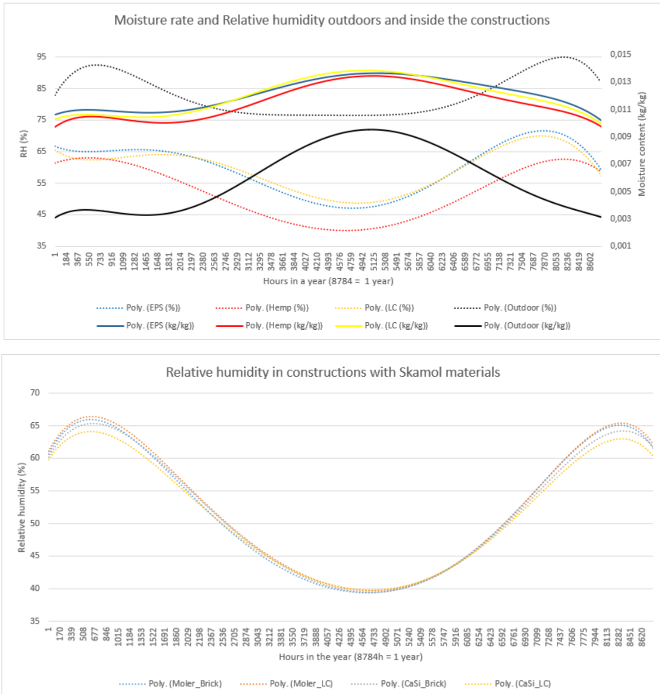

Figure 18 - Yearly mean RH and moisture content

Another factor to distinguish dissimilarity between moisture permeable and non-permeable construction is the indoor RH amplitude among cycles with and without moisture generation (so called moisture buffer potential [51]). Therefore, separate model is created with 16 [h] of moisture generation and 8 [h] of no moisture loads and then reversed. The ventilation system is disabled, rest input parameters stays as in previous simulations. The lower amplitude, the better buffering abilities of the material, as by passively absorbing and releasing moisture, the fluctuations are damped. Simulation is performed on 3 days only (14-17.11.20) and results in following outcomes for EPS and Hempcrete house on Table 8:

Table 8 - Mean and amplitude of RH

	Hemp 16h	EPS 16h	EPS 8h	Hemp 8h
Mean RH (%)	90,8	92,5	79,5	78,9
Min RH (%)	80,0	71,4	53,5	68,1
Max RH (%)	97,4	100,0	100,0	94,5
Amplitude	17,4	28,6	46,6	26,3

The hempcrete construction not only prevents reaching 100 [%] RH but has 50-60 [%] lower amplitude. In EPS construction the RH drops from 100 [%] to little bit above 50 [%] in just 16 [h], hence whole humidity is diluted and if the value will continue to drop, the indoor climate may become too dry. Hempcrete house pattern on Figure 19 follows the one with hygric materials as in [51], while EPS construction presents sharper and more rapid changes.

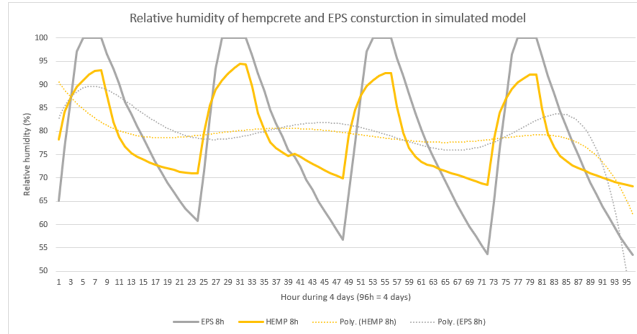

Figure 19 - RH with and without moisture generation

Air change rate has also influence on the RH on hygric materials – low ACH allows hygric material to absorb water particles, hence maintaining steadier RH indoors. When increasing the ACH, the ventilated space is supplied with fresh, less humid air and moisture content indoors is not entering deeply in porous hygric construction, as it is being extracted with the return air, similarly as within non-water permeable constructions, neglecting the buffering effect. That can be seen in Table 9 where mean RH along with amplitude drops with increased ACH. Although the hygric materials still have better conditions, the effect is not that significant.

Table 9 - Mean RH and amplitude at different ACH

ACH	**0.57**	**1.07**	**2.07**
Construction		**Mean RH over a year**	
EPS	59.8	50.5	46.2
LC	59.6	50.8	46.5
Hempcrete	52.1	46.9	44.7
CaSi LC	51.6	46.5	44.6
CaSi Brick	52.0	46.7	44.6
Moler LC	52.5	46.7	44.6
Moler Brick	52.2	46.7	44.5
Construction		**Amplitude**	
EPS	34.4	26.3	26.4
LC	27.8	24.2	22.4
Hempcrete	24.6	23.5	20.1
CaSi LC	26.7	23.3	20.8
CaSi Brick	27.4	23.4	21.1
Moler LC	31.3	24.4	23.6
Moler Brick	31.1	24.4	23.6

IV. Conclusion

Material scale experiments were performed to assess thermal and hygric properties of selected materials. Measured parameters are to some extent comparable with literature and data from the manufacturer and used in dynamic simulation. Moreover, calculated MBV_{ideal} presents excellent outcomes for HH (3.12 [g/m^2%RH]) and CaSi (3.32 [g/m^2%RH]) materials, however $MBV_{practial}$ is necessary to confirm the calculation. Application of investigated renders limits moisture permeability of specific materials of 3-18 [%], but due to large deviations further tests are required to determine actual effect. Calculated retardation factor based on Cup Method and ODA20 indicates larger differences than in [29], being 1106 for CaSi and 1173 for HH. For more accountable outcomes measurements at different RH are recommended. Simulated indoor environment confirms moisture buffering abilities of analysed hygric materials and passive indoor moisture regulation, hence presenting benefits of applying them. That includes lower amplitude of RH variations, greater number of hours in Cat I for RH and preventing the investigated area to reach 100 [%] RH indoors. For an ACH of 0.5 [h^{-1}] the RH peaks are decreased from 92 (EPS) to 73 [%] (hempcrete). Moreover, CaSi board and Moler brick can be used as interior cladding in modern buildings to reduce indoor RH fluctuations. Construction having largest moisture buffering performance is high-hempcrete with low-hempcrete as a render, due to great hygric properties and its application on whole external wall.

V. References

[1] G. C. P. O. F. Lei Fang, Temperature and humidity: important factors for perception of air quality and for ventilation requirements. Issue number Pt. 2, Pages (from-to) 503-510, A S H R A E Transactions, 2000.

[2] C. W. R. L. P. P. N Mendesa, »Moisture effects on conduction loads,« Elsevier Science B.V., 2002.

[3] L. F. G. C. P. O. Fanger, »Impact of Temperature and Humidity on Perception of Indoor Air Quality During Immediate and Longer Whole-Body Exposures,« Volume 8, Issue 4, Pages: 203-301, 1998.

[4] C. R. C. M. S. F. P. C. Y. d. K. V. G. M. E. d. O. F. J. B. P M Bluyssen, »Self-reported health and comfort in 'modern' office buildings: first results from the European OFFICAIR study,« *National Center for Biotechnology Information* , 2015.

[5] M. Q. C. R. Z. C. Mingjie Zhang, »Moisture buffering phenomenon and its impact on building energy consumption,« Applied Thermal Engineering, Volume 124, September 2017, Pages 337-345, Nanjing, China & Lyngby, Denmark, 2017.

[6] S. R. Hans Janssen, »Qualitative and quantitative assessment of interior moisture buffering by enclosures,« Elsevier B.V. Energy and Buildings (Volume 41, Issue 4, April 2009, Pages 382-394), 2008.

[7] Q. M. Z. M. Wu Zhimin, »Phase change humidity control material and its impact on building energy consumption,« 2018 Elsevier B.V. Energy and Buildings (Volume 174, 1 September 2018, Pages 254-261), 2018.

[8] H. Y. K. H. J. L. W. Z. H. X. Huibo Zhang, »Practical moisture buffering effect of three hygroscopic materials in real-world conditions,« 2017 Elsevier B.V. Energy and Buildings (Volume 139, 15 March 2017, Pages 214-223), 2017.

[9] D. Z. K. S. H.M. Kunzel, »Predicting Indoor Temperature and Humidity Conditions Including Hygrothermal Interaction with the Building Envelope,« 1st International Conference on Sustainable Energy and Green Architecture, Building Scientific Reaser Center (BSRC), King Mongkut's Univeristy, Bangkok, 2003.

[10] C. J. S. Olalekan F.Osanyintola, »Moisture buffering capacity of hygroscopic building materials: Experimental facilities and energy impact,« Energy and Buildings pages 1270-1282, Saskatoon, 2006.

[11] M. L. A. S. P. W. Eshrar Latif, »Moisture buffer potential of experimental wall assemblies incorporating formulated hemp-lime,« Building and Environment Pages 199-209, Bath, 2015.

[12] M. E. M. D. O. A. M. K. Hanifi Binici, »An environment-friendly thermal insulation material from sunflower stalk, textile waste and stubble fibers,« Construction and Building Materials 51:24–33, Kahramanmaras & Mersin, 2014.

[13] S. P. Florence Collet, »Thermal conductivity of hemp concretes: Variation with formulation, density and water content,« *Science Direct - Construction and Building Materials* , 2014.

[14] S. P. R. Walker, »Moisture transfer and thermal properties of hemp–lime concretes,« *Science Direct - Construction and Building Materials* , 2014.

[15] S. P. Florence Collet, »Thermal conductivity of hemp concretes: Variation with formulation, density and water content,« *Elsevier - Constructions and Building Materials*, 2014.

[16] A. Evrard, »Transient hygrothermal behavior of Lime-Hemp Materials,« *ResearchGate* , 2008.

[17] S. Pavía, »The impact of water retainers in hemp-lime concrete with pozzolans,« *ResearchGate*, 2013.

[18] J. C. S. P. C. L. Florence Collet, »Comparison of the hygric behaviour of three hemp concretes,« *ELSEVIER - Energy and Buildings* , 2013.

[19] M. B. L. S. J. M. Florence Collet *, »Porous structure and water vapour sorption of hemp-based materials,« *ELSEVIER - Construction and Building Materials* , 2007.

[20] F. C. S. P. J. C. Brahim Mazhoud, »Hygric and thermal properties of hemp-lime plasters,« *ELSEVIER - Building and Environment*, 2015.

[21] S. P. Florence Collet, »Experimental investigation of moisture buffering capacity of sprayed hemp concrete,« *ELSEVIER - Construction and Building Materials* , 2012.

[22] Skamol, »SkamoWall,« Skamol Group, [Online]. Available: https://www.skamowall.com/. [Senest hentet eller vist den 02 10 2020].

[23] Skamol, »Moler and diatomite,« Skamol Group, [Online]. Available: https://www.skamol.com/about/production/materials/moler-and-diatomite. [Senest hentet eller vist den 02 10 2020].

[24] U. R. P. H. John Grunewald, »The Rijksmuseum Amsterdam - Hygrothermal analysis and dimensioning of thermal insulation,« Syracuse University, & Dresden University of Technology, New York & Dresden, 2006.

[25] Y. I. Antonov, »Experimental Characterization of Hemp-Lime Building Material,« 2016.

[26] D. I. 12572:2016, »Hygrothermal performance of building materials and products – Determination of water vapour transmission properties –Cup method,« Dansk Standard, Copenhagen, 2016.

[27] E. S. N. E. E. NORM, »EN 12086:2013 Thermal insulating products for building applications - Determination of water vapour transmission properties,« CEN, Brussels, 2013.

[28] I. O. f. Standardization, »ISO 12572:2016 Hydrothermal performance of building materials and products - Determination of water vapor transmission properties - Cup method,« CEN, Brussels, 2016.

[29] Y. I. A. H. J. P. M. R. L. J. Kirstine Meyer Frandsen, »Experimental investigation of water vapor diffusivity in bio-based building materials by a novel measurement method,« RN4L2020 International Conference, Paper number: 137, Cambridge, UK, 2020.

[30] P. R. M. L. Rode C, »Moisture buffering of building materials.,« Department of Civil Engineering, DTU, Kongens Lyngby, 2005.

[31] R. P. B. T. K. S. a. T. O. Carsten Rode, »Moisture Buffer Value of Building Materials,« Journal of ASTM International, Vol. 4, No. 5, West Conshohocken, 2007.

[32] Greenspec, »Plaster and Render,« Greenspec, [Online]. Available: https://www.greenspec.co.uk/building-design/plaster-and-render/. [Senest hentet eller vist den 17 10 2020].

[33] H. Künzel, »Die ”klimaregelnde wirkung” von innenputzen,”,« GesundheitsIngenieur 81 7 196–201, 1960.

[34] P. J. Paulien Strandberg-de Bruijn, »Moisture transport properties of lime-hemp concrete determined over the complete moisture range,« *ELSEVIER*, 2014.

[35] E. M. Trine Østergaard Jensen, »Fungal Resistance of Calcium Silicate Boards,« DTU, Taastrup, 2015.

[36] H. M. Tommerup, »Energy performance of Moler bricks,« Rambøll, København, 2017.

[37] I. U. O. P. A. A. CHEMISTRY, »REPORTING PHYSISORPTION DATA FOR GAS/SOLID SYSTEMS with Special Reference to the Determination of Surface Area and Porosity,« 1984.

[38] I. Decagon Devices, »Vapor soprtion analyzed (VSA) operator's manual,« AquaLab, Pullman WA 99163, 2017.

[39] M. Q. C. R. Z. C. Mingjie Zhang, »Moisture buffering phenomenon and its impact on building energy consumption,« Applied Thermal Engineering 124 (2017) 337-345, Lyngby / Nanjing, 2017.

[40] K. C. M. Marc Olivier Abadie, Moisture performance of building materials: From material characterization to building simulation using the Moisture Buffer Value concept, Curitiba, Brazil; La Rochelle, France: Pontifical Catholic University of Paraná, LEPTAB - University of La Rochelle, 2008.

[41] B. a. H. Ministry of Transport, »Building Regulation 2018,« Ministry of Transport, Building adn Housing, København, 2017.

[42] A. A. J. K. B. O. Kaiser Ahmed, »Occupancy schedules for energy simulation in new prEN16798-1 and ISO / FDIS 17772-1 standards,« Elsevier, Sustainable Cities and Society, 2017.

[43] M. J. K. S. G. BLUMCHEN, »Metabolic Equivalents (METS) in Exercise Testing, Exercise Prescription, and Evaluation of Functional Capacity,« Clin. Cardiol. 13, 555-565, Ottawa, Ontario, 1990.

[44] A. E. Swiniarski, »Indoor environment conditions and energy performance of a residential building constructed in SIP technology - computer simulations and measured parameters comparison,« Aalborg University, Aalborg, 2018.

[45] A. Moropoulou, M. Karoglou, A. Giakoumaki, M. Krokida, Z. Maroulis og G. Saravacos, »Drying kinetics of some building materials,« National Technical University of Athens, Athens, Greece, 2005.

[46] J. F. Straube, »Moisture control and enclosure wall systems,« University of Waterloo, Waterloo, Canada, 1998.

[47] R.Miniotaite, »Sorption processes and moisture deformations in building materials,« Kaunas University of Technology, Kaunas, Lithuania .

[48] O. A. T. L. G. T. L. M. Rahim, »Moisture properties of rape straw concrete and hemp concrete,« First International Conference on Bio-based Building Materials, Amiens Cedex, 2015.

[49] K. C. M. Marc Abadie, »Moisture performance of building materials: From material characterization to building simulation using the Moisture Buffer Value concept,« Pontifical Catholic University of Paraná, Curitiba, 2009.

[50] O. Koronthalyova, »The coupled effect of hygroscopic materials and ventilation regime on indoor humidity,« IEA-EXCCO Energy Conservation in Buildings and Community Systems ANNEX 41 Kyoto meeting, Institute of Construction and Architecture, SAS, Slovakia .

[51] H. G. P. F. a. J. R. Xiangjin Yang, »Evaluation of Parameters Influencing the Moisture Buffering Potential of Hygroscopic Materials with BSim Simulations,« ISSN 2075-5309, Canada, 2014.

[52] S. H. R. J. T. K. Hyeun Jun Moon, »The effect of moisture transportation on energy efficiency and IAQ in residential buildings,« Elsevier, Yongin , 2014.

[53] D. A. T. P. P. W. M. L. Dr Daniel Maskell, »Determination of optimal plaster thickness for moisture buffering of indoor air,« BRE Centre for innovative Construction Materials, Department of Architecture and Civil Engineering,, Bath, 2017.

[54] E. T. M. V. T. R. J. V. Olli Tuominen1, »Thermal and moisture properties of calcium silicate insulation

boards,« MATEC Web of Conferences 282, CESBP , Tampere,, 2019.

[55] J. Straube, »Moisture Properties of Plaster and Stucco for Strawbale Buildings,« EBNet .

VI. Appendix

Appendix A – Hempcrete material
Appendix B – Skamol materials
Appendix C – LFA (thermal diffusivity and Cp)
Appendix D – VSA (sorption isotherms)
Appendix E – Dry Cup method (moisture permeability)
Appendix F – ODA20 (moisture permeability)
Appendix G – BSim simulation – input and results
Appendix H – Data from IC meter
Appendix I – Calculations (MBV, Pd, moisture effusivity)